Journal of Geointerface, Vol. 5, No. 1, July 2026, pp. 50–59 e-ISSN: 2583-6900

Peak-metamorphic conditions derived from conventional geothermobarometry and pseudosection modelling of enderbites from the southeastern Madurai Block, southern India

G. Indu*, E. Shaji, R.B. Binojkumar

Department of Geology, University of Kerala, Kariavattom Campus, Thiruvananthapuram 695 581, Kerala, India

ABSTRACT

The mineral chemistry using Electron Probe Micro Analysis (EPMA) is a powerful tool for establishing the pressure-temperature (P-T) conditions of a metamorphic terrain. The study area, The Madurai Block, a pivotal component of the Southern Granulite Terrain (India), preserves a complex record of high-grade metamorphism linked to the assembly of the Gondwana supercontinent. However, the precise pressure-temperature (P-T) evolution of its northern, central, and southern sub-blocks remains ambiguous. This study presents a detailed petrological and mineral-chemical investigation of enderbites from the Southeastern Madurai Block to quantify their metamorphic history. Mineral chemistry data, acquired by EPMA, were utilised for conventional geothermobarometry, constraining peak P-T conditions of 6–8.4 kbar and 840–900 °C. Phase-equilibrium modelling in the NCKFMASHT system for a representative sample confirms the stability of the peak assemblage within this medium-pressure, high-temperature granulite-facies field. The modelling further reveals that the mineral paragenesis is robust and insensitive to variations in water activity, indicating fluid-absent conditions during peak metamorphism. Our results demonstrate that the Southeastern Madurai Block experienced regional high-temperature metamorphism under an elevated thermal gradient, distinctly higher than those recorded in other domains of the Southern Granulite Terrain. These quantitative P-T constraints provide critical new data for unravelling the differential tectonic evolution and final assembly of the Gondwana supercontinent.

ARTICLE HISTORY

Received: 27 Nov 2025
Revised: 10 Feb 2026
Accepted: 11 Feb 2026

https://doi.org/10.5281/zenodo.18608368

KEYWORDS

Southern Granulite Terrain (SGT)
Madurai Block (MB)
Ultra-high-temperature (UHT) metamorphism
EPMA
Pseudosection

1. Introduction

The Indian Shield represents a complex mosaic of Archean cratonic nuclei, including the Aravalli-Bundelkhand, Dharwar, Bastar, and Singhbhum cratons, encircled by Proterozoic orogenic belts that archive a protracted geologic history from the Eoarchean/Paleoarchean onwards (Patranabis-Deb et al., 2020). The southernmost segment of this shield, the Southern Granulite Terrain (SGT), is particularly significant as it preserves a critical record of tectonic processes related to the assembly and disintegration of the Gondwana supercontinent (e.g., Collins et al., 2014; Santosh et al., 2009, 2015; Plavsa et al., 2014).

The SGT itself is a composite of several crustal blocks—such as the Coorg, Nilgiri, Salem, Madras, Madurai, Trivandrum, and Nagercoil Blocks-separated by major crustal-scale shear and suture zones (Fig. 1). These tectonic boundaries range in age from the Mesoarchean to the Neoproterozoic-Cambrian, reflecting multiple episodes of accretion and amalgamation. The blocks north of the Palghat-Cauvery Suture Zone (PCSZ) were assembled mainly during the Archean and accreted to the Dharwar Craton, while those to the south were primarily accreted

*Corresponding author. Email: indug2025@keralauniversity.ac.in (GI), shajigeology@gmail.com (SE)

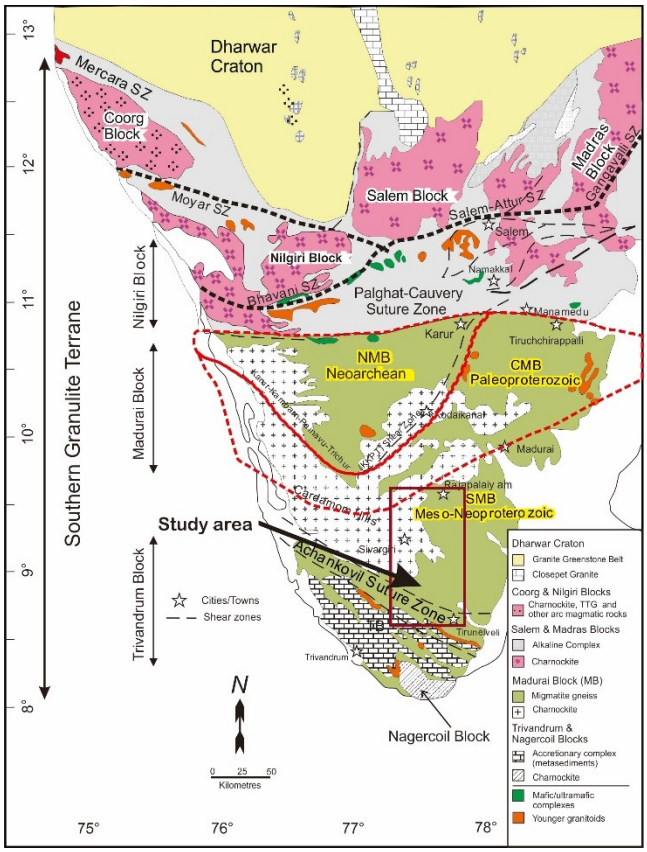

Fig. 1. Generalised geological and tectonic framework of the Southern Granulite terrain of India showing the major crustal blocks and intervening suture zones (after Collins et al., 2014; Santosh et al., 2015). The tectonic subdivision of the Madurai Block is modified after Plavsa et al. (2012, 2014).

during the Neoproterozoic-Cambrian, coinciding with the final assembly of Gondwana (Santosh et al., 2009; Collins et al., 2014; Samuel et al., 2014).

Among these, the Madurai Block (MB) is an important crustal unit and has been the focus of extensive research concerning its petrology, crustal evolution, and tectonism (e.g., Harris et al., 1996; Braun and Appel, 2006; Chatterjee et al., 2024; Gao et al., 2022; García-Arias and Stevens, 2017; Mayne et al., 2016; Santosh et al., 2017). Traditionally regarded as a single entity, recent geochronological and structural studies have proposed a tripartite subdivision into the Northern (NMB), Central (CMB), and Southern (SMB) Madurai blocks (Plavsa et al., 2012, 2014; Santosh et al., 2015). Despite this advanced understanding, the precise petrological character, the pressure-temperature-time (P-T-t) evolution of these individual sub-blocks, and the mechanisms of their final assembly into a unified block remain poorly constrained. Resolving these details is crucial not only for deciphering the tectonic evolution of the SGT but also for correlating these events with those recorded in other Gondwana fragments.

Numerous studies have documented Ultra-High-Temperature (UHT) metamorphism within the Madurai Block, with peak conditions exceeding 900–1000 °C. Key evidence includes mineral assemblages such as sapphirine + quartz and sapphirine + cordierite ± corundum, reported from various localities including Rajapalayam and Usilampatti (e.g., Tsunogae and Santosh, 2003; Tateishi et al., 2004; Prakash and Arima, 2003). However, the precise Pressure-Temperature-time (P-T-t) evolution remains debated, with studies proposing both clockwise (e.g., Prakash et al., 2007; Li et al., 2019) and counterclockwise (Tsunogae and Santosh, 2011) P-T paths.

This study focuses on the southeastern part of the Madurai Block to quantitatively constrain its metamorphic history. We employ detailed petrographic and mineral-chemical analysis of enderbites using Electron Probe Micro-Analysis (EPMA) on key mineral assemblages. Compositional data from minerals such as orthopyroxene, plagioclase, and feldspars are used in conventional geothermobarometry. Furthermore, we utilise phase equilibrium modelling

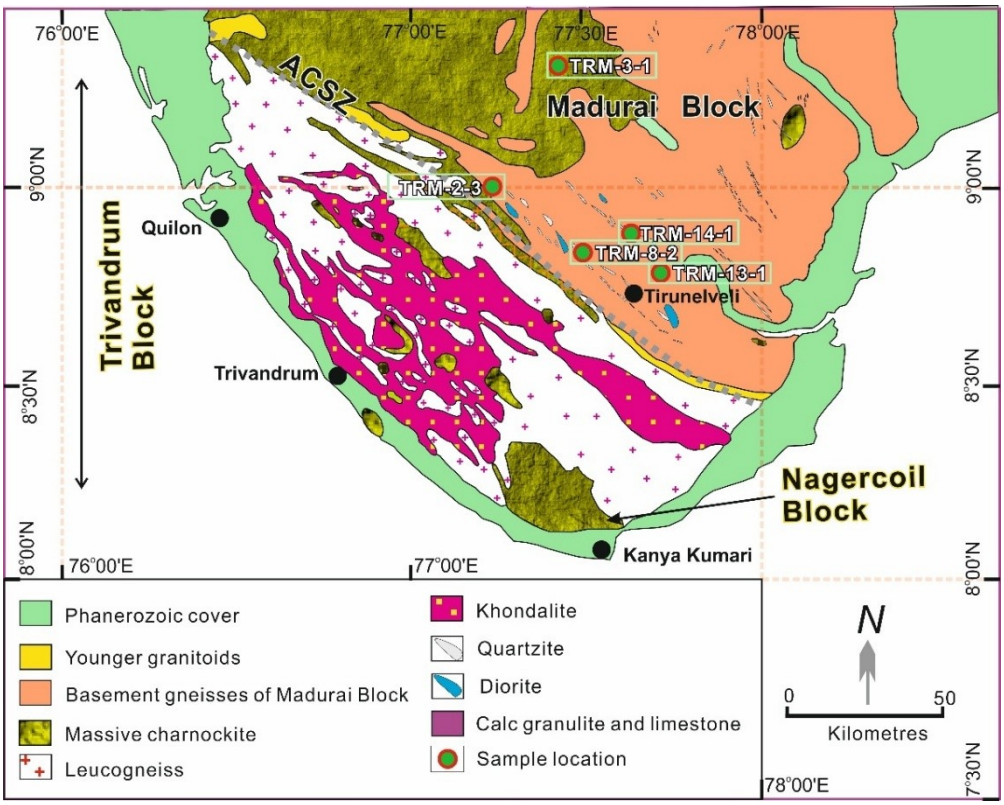

Fig. 2. Detailed geological map of the study area showing sample locations.

(pseudosection analysis) in the NCKFMASHT system to delineate the precise P-T conditions of the peak metamorphism.

2. Geologic setting and petrology

The study area falls in the state of Tamil Nadu, South India, and covers the Tirunelveli, Tuticorin, and Virudhnagar districts, which form the southeastern part of the southern Madurai Block. The study area is located between 9°28′48.38″ N to 8°30′20.5″ N and 77 ° 3′44.84″ E to 77 ° 8′57.97″ E with an area of 5623 sq. km. The Survey of India topographic sheet numbers 58 H/9 and 58 H/14 were used to prepare a base map of the study area. The rock units of the southeastern Madurai Block margin comprise high-grade metamorphic and intrusive suites, notably massive charnockites, migmatitic TTG gneisses, metapelitic bands, metacarbonates, and younger felsic intrusions (Fig. 2). Quartzites are also present in the study area, which forms folded linear ridges and mounds, as well as conformable bands within garnet-biotite sillimanite gneisses.

At many locations, the charnockites look more felsic and are intermediate in composition and are therefore named as enderbites (Fig. 3a). Enderbitic rocks show foliation with visible clots of orthopyroxene and laths of biotite oriented parallel to the foliation. Garnet is absent in these rocks. The enderbitic host rocks carry medium to fine-grained enclaves of dioritic rocks and thin stretched layers and lenses of hornblendite in some locations (Fig. 3b). Several well-cuttings expose the enderbites, which are mostly medium-grained, massive, with clots and layers of orthopyroxene. Five locations are noted for the enderbite samples (Fig. 2). Enderbite sample locations with GPS reading and their mineral assemblages are represented in Table 1.

Most of the enderbites contain abundant plagioclase (40–50%) and quartz (20–30%) with subordinate orthopyroxene (5–10%), K-feldspar (5–10%), biotite (2–5%), zircon (<1%), and apatite (<1%). It is characterised by coarse-grained, subidioblastic to xenoblastic, pleochroic, inclusion-free orthopyroxene, surrounded by rounded plagioclase and quartz. K-feldspar is present only as interstitial grains mostly between matrix plagioclase and quartz. Medium to fine-grained reddish-brown flakes of biotite occur adjacent to orthopyroxene grains, possibly formed by the following hydration reaction

$$\mathrm{Opx + Kfs + H_2O => Bt + Qtz} \quad (1)$$

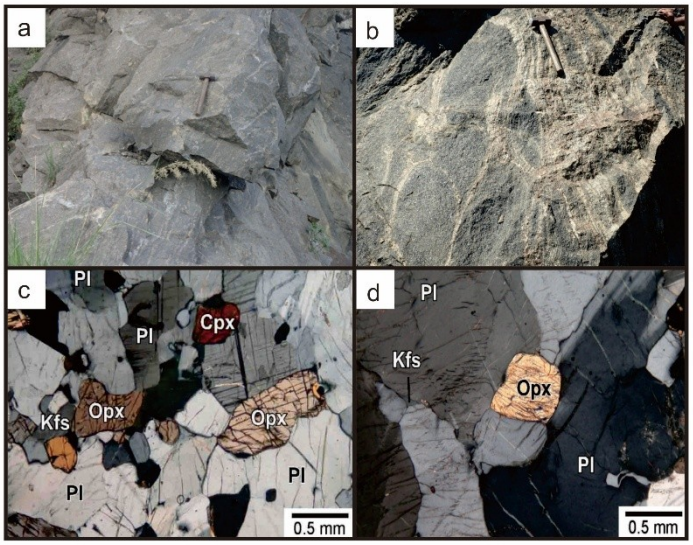

Fig. 3. (a) Enderbite exposure located in Shenkottai (b) Dark coloured dioritic enclaves observed within enderbite (c) Enderbite with mineral assemblages of orthopyroxene, clinopyroxene, plagioclase feldspar and potash feldspar showing granoblastic texture (d) Subhedral orthopyroxene in the matrix of coarse-grained plagioclase in enderbite sample.

Table 1. List of enderbite sample locations with GPS reading and mineral assemblage.

Serial Number	Sample Number	Rock Type	Sample Location	Coordinates	Mineral Assemblage
1	TRM 2-3	Enderbite	Chenkottai	N 08°59′27.56″ E 77°14′15.10″	Pl + Kfs + Qtz + Opx + Bt + Ap + Zr
2	TRM 3-1	Enderbite	Sivagiri	N 09°21′04.06″ E 77°26′25.55″	Pl + Kfs + Qtz + Opx + Bt + Ap + Zr
3	TRM 8-2	Enderbite	Karumpuliyutl	N 08°50′07.71″ E 77°31′53.74″	Pl + Kfs + Qtz + Hbl + Il + Ap + Bt
4	TRM 13-1	Enderbite	Thalayuth	N 08°48′09.52″ E 77°43′20.57″	Pl + Kfs + Qtz + Opx + Cpx + Hbl + Il + Ap + Zr
5	TRM 14-1	Enderbite	Kaanarpetti	N 08°53′18.48″ E 77°38′28.15″	Pl + Kfs + Qtz + Opx + Hbl + Mt. + Ap + Zr

Some samples carry very coarse-grained subhedral orthopyroxene. It shows a typical granoblastic texture of plagioclase (60–70%), quartz (20–30%) and orthopyroxene (5–10%). Interstitial K-feldspar is also present in some of the samples and plagioclase rich and clinopyroxene-bearing enderbites have plagioclase (55–65%), K-feldspar (10–25%), orthopyroxene (10–15%), clinopyroxene (2–5%), quartz (2–5%), and Fe–Ti oxide (1–2%) (Fig. 3c).

Minor calcic amphibole is also present in one sample (< 1%). Both orthopyroxene and clinopyroxene are subhedral to rounded, rarely anhedral, and occur as aggregates forming pyroxene-rich domains. Subhedral orthopyroxene in the coarse-grained plagioclase matrix is common (Fig. 3d). Plagioclase and quartz are semi-granoblastic and subhedral, while K-feldspar occurs as fine- to medium-grained interstitial grains.

3. Methodology

3.1. Sample Preparation

Doubly polished thin sections of the representative samples (enderbite) were prepared in the Continental Instruments, Lucknow. The standard size of the polished sections is 45–47 mm in length, 25 mm in width, and 0.03 mm in thickness, and they are mounted on epoxy.

3.2. Analytical technique

Polished thin sections of sample TRM 2–3 were examined in detail under a petrographic microscope, then imaged by backscattered electrons (BSE) and mineral compositions measured using a JEOL JXA 8230 electron microprobe at the Advanced Facility for Microscopy and Microanalysis (AFMM), Indian

Table 2. Representative compositions of minerals in enderbite samples obtained by EPMA.

Sample No.	TRM 13-1	TRM 8-2	TRM 14-1	TRM 2-3	TRM 14-1	TRM 2-3	TRM 3-1	TRM 8-2
Mineral Name	Pl	Pl	Pl	Pl	Kfs	Kfs	Kfs Lamella	K-fs
SiO_2	62.78	61.76	60.98	61.14	63.81	64.21	64.47	63.55
Al_2O_3	23.37	21.76	24.49	24.05	18.61	18.6	18.64	17.23
TiO_2	0.02	0.01	0.02	0	0.02	0.05	0.02	0.04
Cr_2O_3	0	0.01	0.03	0	0	0.01	0	0
FeO*	0.2	0.06	0.14	0.04	0.07	0.01	0	0.08
MnO	0	0.02	0.01	0.02	0	0	0	0
MgO	0.02	0.01	0	0	0	0	0	0
CaO	4.85	5.52	6.33	6.01	0.04	0.17	0.06	0.16
Na_2O	8.16	10.21	7.32	7.71	0.4	0.66	0.51	2.07
K_2O	0.75	0.42	0.56	0.71	15.41	15.17	15.6	16.3
Total	100.15	99.78	99.89	99.69	98.36	98.87	99.3	99.43
An%	23.7	22.5	31.3	28.9	0.2	0.9	0.3	0.7
Ab%	72	75.4	65.4	67.1	3.8	6.1	4.7	16.1
Or%	4.4	2	3.3	4	96	93	95	83.2
Sample No.	TRM 2-3	TRM 3-1	TRM 14-1	TRM 8-2	TRM 2-3	TRM 3-1	TRM 8-2	
Mineral Name	Opx	Opx	Opx	Opx	Bt	Bt	Bt	
SiO_2	47.77	50.1	52.09	48.01	37.09	36.12	36.54	
Al_2O_3	6.97	0.79	1	4.17	15.13	13.22	14.12	
TiO_2	0.21	0.12	0.1	0.11	5.01	3.1	5.12	
Cr_2O_3	0.01	0.07	0.01	0	0.01	0.06	0.04	
FeO*	24.66	30.91	24.48	27.01	12.36	20.85	15.7	
MnO	0.53	0.7	0.84	1.07	0.12	0.06	0.09	
MgO	18.98	15.25	20.43	19.13	15.42	10.88	15.27	
CaO	0.09	1.51	0.63	0.14	0	0.07	0.09	
Na_2O	0.04	0.04	0	0.02	0.03	0.03	0.07	
K_2O	0	0	0	0.01	9.77	8.96	11.21	
Total	99.26	99.48	99.58	99.67	94.94	93.35	98.25	
Mg/(Fe + Mg)	0.58	0.47	0.6	0.35	0.69	0.48	0.63	
yOpx**	0.13	0.005	0.018	0.17				
Sample No.	TRM 14-1	TRM 14-1	TRM 13-1	TRM 2-3	TRM 2-3	TRM 8-2		
Mineral Name	Hbl	Mt	Mt	Ilm	Qtz	Qtz		
SiO_2	43.46	0.02	0.01	2.852	99.73	99.29		
Al_2O_3	9.93	0.9	0.82	1.501	0.05	0.01		
TiO_2	1.63	0.76	0.35	64.09	0.01	0.04		
Cr_2O_3	0.03	0.13	0.12	0.04	0.02	0		
FeO*	14.65	96.94	98.11	25.87	0.01	0.15		
MnO	0.18	0.15	0.05	0.84	0	0		
MgO	12.04	0.02	0.02	0.43	0	0		
CaO	11.75	0.01	0	0.31	0.01	0.04		
Na_2O	1.28	0.04	0.04	0.12	0.03	0.06		
K_2O	1.56	0.01	0	0.07	0.01	0.04		
Total		98.98	99.52	96.123	99.87	99.63		

Institute of Science, Bangalore. The analytical conditions for the analyses were a beam diameter of 3 m, an accelerating potential of 15 kV, and a probe current of 12 nA. Count times for the major elements were 10 s on the peaks and 5 s on each background. Natural silicate and oxide minerals were used for calibration. Data were processed with a ZAF-type correction. Representative mineral compositions are listed in Table 2.

3.3. Geothermobarometry

Geothermobarometric analysis was carried out to constrain the metamorphic conditions of the rocks from the study area using EPMA-derived mineral compositional data. Appropriate geothermometers and geobarometers applicable to felsic to intermediate charnockitic compositions were employed. The calculations are based on established activity-composition relationships for relevant mineral equilibria among major rock-forming phases, ensuring internal consistency between mineral chemistry and equilibrium assumptions. Multiple thermometer-barometer calibrations were applied to assess the robustness and reproducibility of the calculated conditions. The results obtained from these calculations were subsequently evaluated in conjunction with petrographic observations and mineral equilibrium modelling.

3.4. Mineral Equilibrium Modelling

Metamorphic P-T conditions and the stability of mineral assemblages in the enderbite sample TRM 2-3 from Shenkottai were constrained using THERMOCALC version 3.33 (Powell et al., 1998; updated October 2009) with the internally consistent thermodynamic dataset of Powell et al. (1998) (dataset TCDS55s, file created November 2003). The calculations are based on Gibbs free energy minimization, which determines stable mineral assemblages and phase compositions for a given bulk rock composition over a range of pressure-temperature conditions. The resulting outputs were used to construct rock-specific equilibrium assemblage diagrams, commonly referred to as P-T pseudosections.

Pseudosection modelling was carried out in the Na_2O–CaO–K_2O–FeO–MgO–Al_2O_3–SiO_2–H_2O–TiO_2 (NCKFMASHT) system following White et al. (2003, 2007), which provides an appropriate compositional framework for modelling enderbites. Quartz, aluminosilicate phases, and H_2O were treated as pure end-member phases. The bulk rock composition of sample TRM 2-3, expressed in mol%, is: SiO_2 = 58.48, Al_2O_3 = 16.44, FeO = 5.14, MgO = 3.64, CaO = 3.63, Na_2O = 3.39, K_2O = 2.09, and TiO_2 = 1.15. MnO was excluded from the modelling due to its negligible concentration. Within the NCKFMASHT system, Fe–Ti oxides may be represented by rutile or sphene rather than ilmenite or magnetite in the calculated assemblages.

The P-T pseudosection for sample TRM 2-3 (Fig. 5.2) was calculated with a fixed water content of M_{H_2O} = 0.2 mol%. The model predicts stability fields for mineral assemblages dominated by Qtz + Kfs + Pl + Opx + Ilm, with or without melt and magnetite. The presence of melt is limited within the relevant stability fields. The stability field corresponding to the peak mineral assemblage was identified within the pseudosection and used to constrain the pressure-temperature conditions. Additional calculations were performed with higher water contents (up to M_{H_2O} = 1.0 mol%) to evaluate the sensitivity of mineral stability to fluid content. Orthopyroxene displays a wide stability field across the investigated P-T range and is present throughout most calculated assemblages. Petrographic observations were used in conjunction with the modelling results to evaluate dehydration reactions, particularly those involving hornblende breakdown during granulite-facies metamorphism.

4. Results

4.1. Mineral Chemistry

Representative compositions of minerals obtained by electron microprobe analyses are summarised in Table 2 and briefly discussed below.

4.1.1. Pyroxenes

Pyroxenes in the studied enderbites are dominated by orthopyroxene with subordinate clinopyroxene, as illustrated in the En-Fs-Wo quadrilateral (Fig. 4a). Most analysed compositions plot within the low-Ca pyroxene field along the enstatite-ferrosilite join, confirming the dominance of orthopyroxene. At the same time, a minor proportion of analyses extend toward the augite field, indicating the presence of Ca-bearing clinopyroxene. Orthopyroxene compositions are consistently enstatite-rich, with X_{Mg} [Mg/(Mg + Fe)] values ranging from 0.47 to 0.61, with sample TRM 3-1 showing the highest Mg enrichment. Al_2O_3 contents display significant variation (0.6–6.97 wt.%), and the highest Al_2O_3 concentration occurs in sample TRM 2-3, corresponding to yOpx (=Si + Al_2) values up to 0.13 pfu (Fig. 4b). These compositions plot close to the orthopyroxene array typical of metamorphic charnockites (Rajesh et al., 2011), indicating partial metamorphic re-equilibration under granulite facies conditions. Clinopyroxene in the examined samples is uniformly classified as augite, with compositions showing moderate Mg enrichment (X_{Mg} 0.60–0.61), although slightly Fe-rich tendencies are observed in sample TRM 3-1. The mineral is characterised by low Na_2O (0.51–0.58 wt.%) and Al_2O_3 (1.19–1.89 wt.%) contents, suggesting limited incorporation of Na and Al and reflecting crystallisation or equilibration under high-temperature conditions typical of granulite-facies assemblages.

4.1.2. Mica classification

The mica compositions plotted in the Mg–Li versus Fe + Mn + Ti + Al^{VI} diagram predominantly fall within the Fe–Mg mica fields, particularly within the siderophyllite-biotite and Mg-biotite domains, indicating the dominance of Fe–Mg biotite with limited Li enrichment. This distribution reflects the moderate Fe–Mg partitioning characteristic of high-temperature metamorphic assemblages. At the same time, the absence of Li-rich compositions suggests minimal influence of Li-bearing fluids or pegmatitic processes. Biotite compositions further vary with

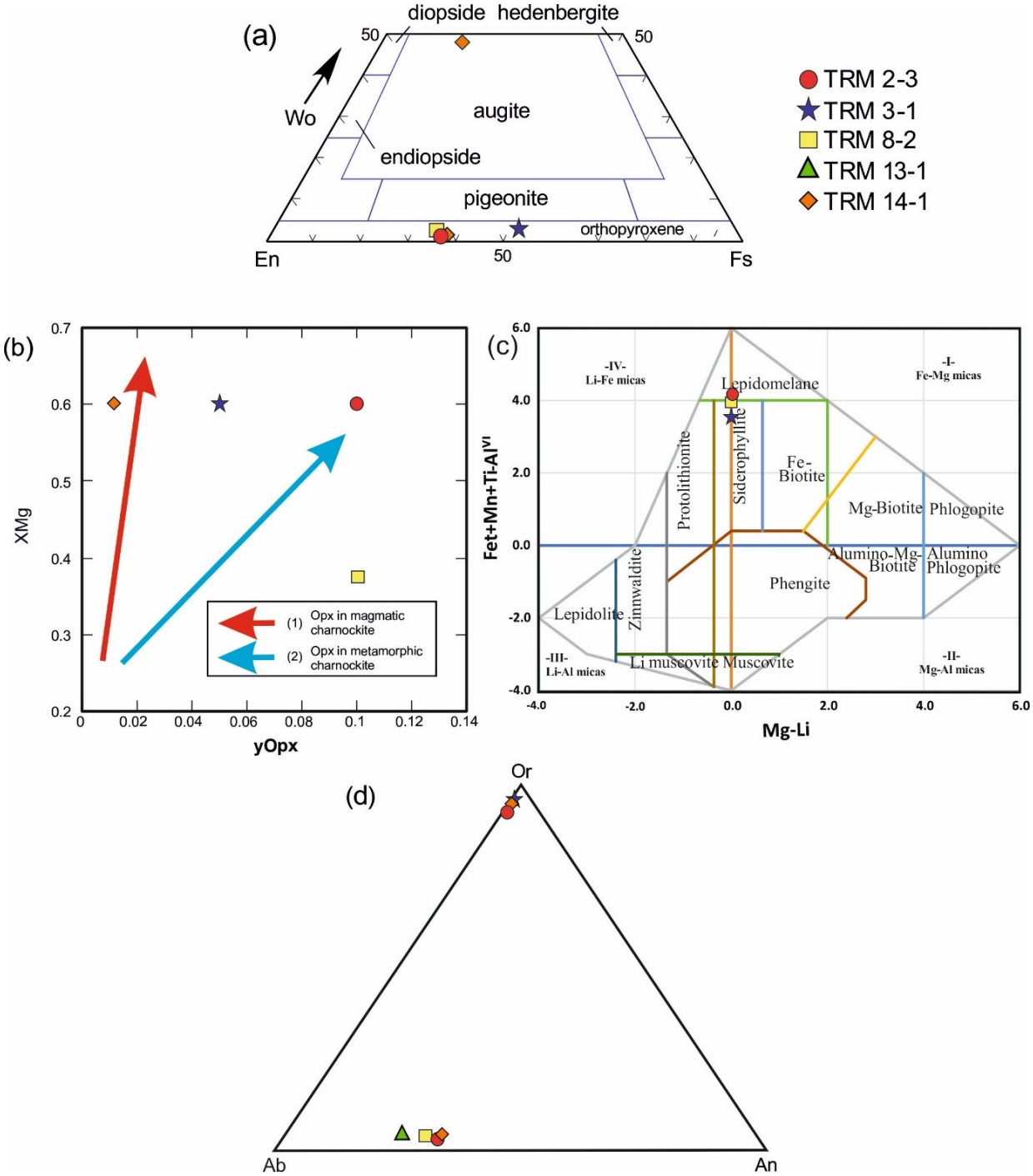

Fig. 4. Compositional diagrams showing the chemistry of representative minerals in enderbites of the study area. (a) Triangular diagram showing pyroxene chemistry (b) yOpx (=Si + Al_2) versus X_{Mg}(=Mg/(Fe + Mg) diagram showing compositions of orthopyroxene. Arrays of magmatic and metamorphic Mg charnockites are after Rajesh et al. (2011) (c) Fet + Mn + Ti–Al^{VI} vs. Mg–Li* classification diagram (Tischendorf et al., 1997) (d) Feldspar chemistry.

rock type (Fig. 4c), with biotite from the enderbite sample TRM 3-1 showing relative depletion in both TiO_2 and Mg, with TiO_2 contents of 3.0–3.1 wt.% and X_{Mg} [Mg/(Mg + Fe)] values of 0.48–0.49. Such variations likely reflect differences in bulk-rock composition and metamorphic re-equilibration conditions, collectively supporting the crystallisation and chemical adjustment of biotite under granulite-facies conditions.

4.1.3. Feldspar classification

Feldspar compositions plotted in the Ab-An-Or ternary diagram define two distinct populations:

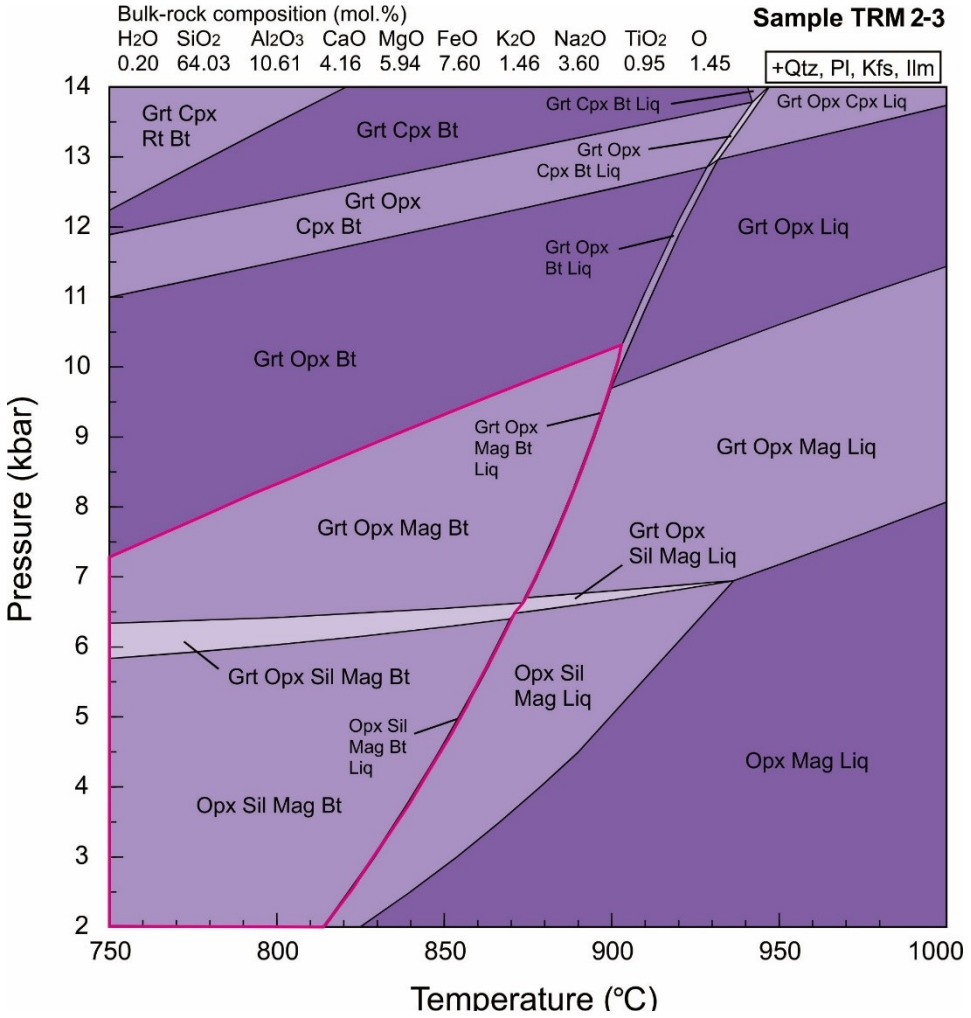

Fig. 5. P-T Pseudosection for sample TRM 2-3 (Enderbite) calculated using the compositional parameters.

one group clustering near the Or apex, corresponding to K-feldspar compositions, and another distributed along the Ab-An join, representing plagioclase feldspar (Fig. 4d). Plagioclase compositions show moderate variation among samples, with enderbites displaying consistent anorthite contents in the range An_{23-31}, while the plagioclase host in sample TRM 3-1 records the highest anorthite content. Despite this variation, the plagioclase compositions remain within the albite-rich field, indicating overall sodic plagioclase dominance with a minor anorthite component. The coexistence of K-feldspar and sodic plagioclase suggests feldspar equilibration at high temperatures typical of charnockitic or granulite-facies assemblages.

4.2. Geothermobarometry and mineral equilibrium modelling

Fig. 5 represents the P-T pseudosection for sample TRM 2-3 (enderbite) calculated using the measured bulk compositional parameters. P-T stability modelling was carried out with water content (M H_2O) fixed at 0.2 mol%. The modelled rock predicts equilibrium assemblages of Qtz + Kfs + Pl + Opx + Ilm, with or without liquid and magnetite, representing the probable peak mineral assemblage. Melt is relatively limited within the stability field of this assemblage, consistent with dry granulite-facies conditions. Although garnet-bearing fields are predicted in parts of the calculated P-T space, garnet is absent in the natural sample. This mismatch is interpreted to reflect kinetic inhibition of garnet nucleation under high-temperature, low-H_2O conditions, coupled with limited availability of reactive Fe–Mg components due to their sequestration in orthopyroxene and Fe–Ti oxides, as well as potential differences between the effective bulk composition and the whole-rock composition used in the modelling. As a result, the preserved mineral assemblage is interpreted to represent a metastable equilibrium attained

during peak metamorphism. The stability field of the garnet-absent peak assemblage in the pseudosection with 0.2 mol% H_2O constrains peak P-T conditions to ~840–900 °C at pressures of ~6–8.4 kbar (see the coloured/hatched area in Fig. 5). Orthopyroxene exhibits a wide stability field and is present throughout the relevant P-T range, supporting its role as a key phase during peak metamorphism. Modelling with higher water contents (e.g., M_{H_2O} = 1.0 mol%) does not produce significant changes in assemblage stability, indicating that variations in fluid pressure had little influence on mineral paragenesis during peak conditions. Petrographic observations further support this interpretation, showing hornblende dehydration within the granulite facies, leading to the formation of enderbites.

5. Discussion

The mineral chemistry of the representative minerals in the rock samples was determined using EPMA. The enderbites from the study area show broadly similar mineralogical constitution of charnockites except for the variation in the modal content of plagioclase, K-feldspar and quartz, as well as the presence of clinopyroxene. To constrain the metamorphic history, pressure-temperature (P-T) conditions were derived from EPMA mineral chemistry. The calculations employed a thermodynamic geothermobarometer that incorporates a calibrated activity-composition model appropriate for the charnockitic composition range of the studied samples.

Phase-equilibrium modelling for sample TRM 2-3 provides robust quantitative constraints on the metamorphic conditions experienced by the enderbites of the Southeastern Madurai Block. The peak metamorphic P-T conditions and stable mineral paragenesis of the enderbite were determined through phase equilibrium modelling using THERMOCALC 3.33. Calculations in the Na_2O–CaO–K_2O–FeO–MgO–Al_2O_3–SiO_2–H_2O–TiO_2 (NCKFMASHT) system, assuming 0.2 mol% H_2O, indicate that the peak assemblage (Qtz + Kfs + Pl + Opx + Ilm) is stable at 840–900 °C and 6–8.4 kbar (Fig. 5). This result is in excellent agreement with the conditions derived from conventional geothermobarometry (this study), confirming a medium-pressure, high-temperature (MP-HT) granulite facies metamorphic event.

6. Conclusions

- EPMA results confirm that the enderbites consist of plagioclase, K-feldspar, quartz, orthopyroxene, and clinopyroxene.
- Geothermometric calculations based on mineral chemistry indicate medium-pressure, high-temperature granulite facies metamorphism.
- Phase equilibrium modelling (THERMOCALC 3.33, NCKFMASHT system) constrains the peak P-T conditions of the enderbites to 840–900 °C and 6–8.4 kbar.
- The peak mineral assemblage (Qtz + Kfs + Pl + Opx + Ilm) is stable within this P-T range, consistent with results from conventional geothermobarometry.

Credit statement

Indu G: Writing – original draft, software, methodology, investigation, funding acquisition, formal analysis, conceptualisation. **Shaji E**: Investigation, supervision, resource mobilisation, data curation, and validation. **Binojkumar R B**: Validation, reviewing, and editing.

Declaration of competing interests

The authors declare that they have no known competing financial interests or personal relationships that could influence the work reported in this paper.

Acknowledgements

Indu G was funded through a Kerala State Council for Science, Technology and Environment (KSCSTE) doctoral scholarship, Government of Kerala, India. The petrography labs of the Department of Geology, University of Kerala, and the EPMA lab of IISc Bangalore have also been utilised for this work.

References

Braun, I., Appel, P., 2006. U-Th-total Pb dating of monazite from orthogneisses and their ultra-high temperature metapelitic enclave implications for the multistage tectonic evolution of the Madurai Block, Southern India. *European Journal of Mineralogy* 18, 415–427. https://doi.org/10.1127/0935-1221/2006/0018-0415.

Chatterjee, S., Mukherjee, S., Sanyal, S., Sengupta, P., 2024. Petrogenesis of magmatic charnockite-biotite granite suite from parts of the Chotanagpur Granite Gneissic Complex (CGGC), eastern Indian shield: Implication for the breakdown of the Columbia Supercontinent. *Lithos* 488, 107802. https://doi.org/10.1016/j.lithos.2024.107802.

Collins, A.S., Clark, C., Plavsa, D., 2014. Peninsular India in Gondwana: The tectonothermal evolution of the Southern Granulite Terrain and its Gondwanan counterparts. *Gondwana Research* 25(1), 190–203. https://doi.org/10.1016/j.gr.2013.01.002.

Gao, S., Cowgill, E., Wu, L., Lin, X., Cheng, X., Yang, R., Yang, S., 2022. From left slip to transpression: Cenozoic tectonic evolution of the North Altyn Fault. *NW margin of the Tibetan Plateau. Tectonics* 41(3). https://doi.org/10.1029/2021TC006962.

García-Arias, M., Stevens, G., 2017. Phase equilibrium modelling of granite magma petrogenesis: An evaluation of the magma compositions produced by crystal entrainment in the source. *Lithos* 277, 131–153. https://doi.org/10.1016/j.lithos.2016.09.028.

Harris, N.B.W., Bartlett, J.M., Santosh, M., 1996. Neodymium isotope constraints on the tectonic evolution of East Gondwana. *Journal of Southeast Asian Earth Sciences* 14(3-4), 119–125. https://doi.org/10.1016/S0743-9547(96)00050-5.

Li, P., Sun, M., Shu, C., Yuan, C., Jiang, Y., Zhang, L., Cai, K., 2019. Evolution of the Central Asian Orogenic Belt along the Siberian margin from Neoproterozoic-Early Paleozoic accretion to Devonian trench retreat and a comparison with Phanerozoic eastern Australia. *Earth-Science Reviews* 198, 102951. https://doi.org/10.1016/j.earscirev.2019.102951.

Mayne, M.J., Moyen, J.F., Stevens, G., Kaislaniemi, L., 2016. Rcrust: a tool for calculating path-dependent open system processes and application to melt loss. *Journal of Metamorphic Geology* 34(7), 663–682. https://doi.org/10.1111/jmg.12199.

Patranabis-Deb, S., Saha, D., Santosh, M., 2020. Tracking India within Precambrian Supercontinent Cycles, in: Gupta, N., Tandon, S. (Eds.), Geodynamics of the Indian Plate. Springer, Cham. https://doi.org/10.1007/978-3-030-15989-4_3.

Plavsa, D., Collins, A.S., Foden, J.F., Kropinski, L., Santosh, M., Chetty, T.R.K., Clark, C., 2012. Delineating crustal domains in Peninsular India: age and chemistry of orthopyroxene-bearing felsic gneisses in the Madurai Block. *Precambrian Research* 198, 77–93. https://doi.org/10.1016/j.precamres.2011.12.013.

Plavsa, D., Collins, A.S., Payne, J.L., Foden, J., Clark, C., Santosh, M., 2014. Detrital zircons in basement metasedimentary protoliths unveil the origins of southern India. *Geol. Soc. Am. Bull* 126, 791–812. https://doi.org/10.1130/B30977.1.

Powell, R., Holland, T.J.B.H., Worley, B., 1998. Calculating phase diagrams involving solid solutions via non-linear equations, with examples using THERMOCALC. *Journal of Metamorphic Geology* 16(4), 577–588. https://doi.org/10.1111/j.1525-1314.1998.00157.x.

Prakash, D., Arima, M., 2003. High-temperature dehydration-melting and decompressive textures in Mg-Al granulites from the Palni Hills, South India. *Polar Geoscience* 16, 149–175. https://doi.org/10.15094/00003127.

Prakash, D., Arima, M., Mohan, A., 2007. Ultrahigh-temperature mafic granulites from Panrimalai, south India: Constraints from phase equilibria and thermobarometry. *Journal of Asian Earth Sciences* 29(1), 41–61. https://doi.org/10.1016/j.jseaes.2006.01.002.

Rajesh, H.M., Santosh, M., Yoshikura, S., 2011. The Nagercoil charnockite: a magnesian, calcic to calc-alkalic granitoid dehydrated during a granulite-facies metamorphic event. *Journal of Petrology* 52(2), 375–400. https://doi.org/10.1093/petrology/egq084.

Samuel, V.O., Santosh, M., Liu, S.W., Wang, W., Sajeev, K., 2014. Neoarchean continent growth through arc magmatism in the Nilgiri Block, southern India. *Precambrian Research* 245, 146–173. https://doi.org/10.1016/j.precamres.2014.02.002.

Santosh, M., Hu, C.N., X.F., Li, S.S., Tsunogae, T, Shaji, E., Indu, G., 2017. Neoproterozoic arc magmatism in the Southern Madurai Block, India: Subduction, relamination, continental outbuilding, and the growth of Gondwana. *Gondwana Research* 45, 1–42. https://doi.org/10.1016/j.gr.2016.12.009.

Santosh, M., Maruyama, S., Sato, K., 2009. Anatomy of a Cambrian suture in Gondwana: Pacific-type orogeny in southern India. *Gondwana Research* 16, 321–341. https://doi.org/10.1016/j.gr.2008.12.012.

Santosh, M., Yang, Q.Y., Shaji, E., Tsunogae, T., Ram Mohan, M., Satyanarayanan, M., 2015. An exotic Mesoarchean microcontinent: the Coorg Block, southern India. *Gondwana Res* 27, 165–195. https://doi.org/10.1016/j.gr.2013.10.005.

Tateishi, K., Tsunogae, T., Santosh, M., Janardhan, A.S., 2004. First report of sapphirine+ quartz assemblage from southern India: implications for ultrahigh-temperature metamorphism. *Gondwana Research* 7(4), 899–912. https://doi.org/10.1016/S1342-937X(05)71073-X.

Tischendorf, G., Gottesmann, B., Förster, H.-J., Trumbull, R., 1997. On Li-bearing micas: Estimating Li from electron microprobe analyses and an improved diagram for graphical representation. *Mineralogical Magazine* 61, 809–834.

Tsunogae, T., Santosh, M., 2003. Sapphirine and corundum-bearing granulites from Karur, Madurai Block, southern India. *Gondwana Research* 6(4), 925–930. https://doi.org/10.1016/S1342-937X(05)71037-6.

Tsunogae, T., Santosh, M., 2011. Sapphirine + quartz assemblage from the Southern Granulite Terrain, India: diagnostic evidence for ultrahigh-temperature metamorphism within the Gondwana collisional orogen. *Geol. J* 46, 183–197. https://doi.org/10.1002/gj.1244.

White, R.W., Powell, R., CLARKE, G.L., 2003. Prograde metamorphic assemblage evolution during partial melting of metasedimentary rocks at low pressures: migmatites from Mt Stafford, Central Australia. *Journal of Petrology* 44(11), 1937–1960. https://doi.org/10.1093/petrology/egg065.

White, R.W., Powell, R., Holland, T.J.B., 2007. Progress relating to calculation of partial melting equilibria for metapelites. *Journal of Metamorphic Geology* 25(5), 511–527. https://doi.org/10.1111/j.1525-1314.2007.00711.x.

